

Imaging Skeletal Pathology in Mutant Mice by Microcomputed Tomography

ALICE F. FORD-HUTCHINSON, DAVID M.L. COOPER, BENEDIKT HALLGRÍMSSON, and FRANK R. JIRIK

ABSTRACT. Objective. We describe the utility of microcomputed tomography (μ CT) for imaging skeletal abnormalities in rodent model systems. For the purpose of illustration, the progressive ankylosis (*ank*) mutant was selected. *ank* mice develop prominent articular and periarticular calcifications at multiple anatomical sites, including paws, elbows, knees, and vertebrae.

Methods. Forelimbs, hindlimbs, and proximal tail vertebrae of 4-month-old female *ank/ank* mice were scanned at 15 μ m resolution using a SkyScan 1072 μ CT instrument and images were generated using Analyze 4.0 software.

Results. This technique was able to show, in 3-dimensional images, the abnormal calcification of *ank/ank* mice, which was readily observed within joint surfaces, on periosteal surfaces, sesamoid bones, menisci, and joint capsules, as well as other periarticular ligamentous structures.

Conclusion. As illustrated by the example of the *progressive ankylosis* mutant, μ CT represents a powerful emerging tool for identifying and monitoring the progression of developmental or acquired skeletal abnormalities within rodent models. (J Rheumatol 2003;30:2659–65)

Key Indexing Terms:

MICROCOMPUTED TOMOGRAPHY PROGRESSIVE ANKYLOSIS ANK MOUSE

Progressive ankylosis (*ank*) is a severe autosomal recessive musculoskeletal disorder of mice characterized by spontaneous fusion of multiple joints secondary to new bone formation and ectopic calcification (hydroxyapatite) within and around the articulations of the limbs and axial skeleton^{1,2}. As a result of this pathology, *ank/ank* mice have a flat-footed gait due to ankle and foot joint fusion, and over time the ankylosis spreads to involve multiple joints in the extremities as well as the vertebral column. The mutant gene responsible for the *ank* phenotype was recently isolated and shown to encode a multipass transmembrane protein, ANK, with a putative role in the transport of pyrophosphate (PPi)². PPi has been shown to function as an inhibitor of mineralization within connective tissue matrices. Indeed, reduced extracellular concentrations of PPi, as are proposed to ensue from a loss of ANK function², have been associated with pathological mineralization in cartilage, periarticular soft

tissues, and bone. Although the *ank/ank* phenotype bears some resemblance to specific forms of osteoarthritis, owing to the occurrence of cartilage erosion, osteophytes, the presence of hydroxyapatite crystal and chondrocalcinosis within affected joints, and vertebral disease¹, the mutation also results in skeletal changes that are reminiscent, yet clearly distinct from, that of a spondyloarthropathy.

Traditionally, skeletal analyses in rodents have been carried out using conventional radiological and histological techniques. With the introduction of microcomputed tomography (μ CT), however, it has become possible to visualize all aspects of the rodent skeleton not only in exquisite detail, but also as 3-dimensional (3-D) images generated with specialized software. A relatively new technology, μ CT has already been applied to various murine models for assessment of changes in trabecular architecture as well as gross morphology^{3–10}. The aim of this study was to employ the *ank* mutant mouse to illustrate the power of μ CT scanning as a way to rapidly obtain detailed information about musculoskeletal pathology in 3-D, while obviating the need for laborious reconstructions based on the examination of multiple histological sections.

MATERIALS AND METHODS

Animals. Mice homozygous for the progressive ankylosis (*ank/ank*) mutation on a C57/BL6 background were obtained from The Jackson Laboratories (Bar Harbor, ME, USA). Controls consisted of two 4-month-old female C57/BL6 mice, as well as 4 additional female mice 7–13 months of age (data not shown). All *ank/ank* mice examined were female, 4 months of age. Mice were maintained in a barrier facility in accord with University of Calgary and Canadian Council on Animal Care guidelines, and euthanized by CO₂ inhalation. In preparation for scanning, limbs were removed at the level of the hip and shoulder joint. The proximal portion of the tail was isolated for intervertebral joint examination. As cryopreservation did

From the Joint Injury and Arthritis Research Group, Department of Biochemistry and Molecular Biology; the Department of Archaeology; and the Department of Cell Biology and Anatomy, University of Calgary, Calgary, Alberta, Canada.

Supported by the Alberta Heritage Foundation for Medical Research (to FRJ) and the Canadian Foundation for Innovation (to BH).

A.F. Ford-Hutchinson, BSc, Graduate Student; F.R. Jirik, MD, FRCPC, Professor, Joint Injury and Arthritis Research Group, Department of Biochemistry and Molecular Biology; D.M.L. Cooper, MSc, Graduate Student, Department of Archaeology; B. Hallgrímsson, PhD, Associate Professor, Joint Injury and Arthritis Research Group, Department of Cell Biology and Anatomy.

Address reprint requests to Dr. F.R. Jirik, Department of Biochemistry and Molecular Biology, University of Calgary, 3330 Hospital Drive NW, Calgary, Alberta T2N 4N1, Canada. E-mail: jirik@ucalgary.ca

Submitted August 14, 2002; revision accepted April 24, 2003.

not significantly alter the μ CT morphology of bone and joint samples (data not shown), all skeletal samples were stored at -20°C prior to analysis.

μ CT analysis. Samples from *ank/ank* mice and controls were scanned using a SkyScan 1072 (Aartselaar, Belgium) x-ray microtomograph, using a cone beam configuration with standardized x-ray tube settings of 100 kV and 100 μA . All appendicular joints were scanned at an isotropic voxel resolution of $15.19\ \mu\text{m}^3$ with an exposure time of 1.3 s and a rotation step of 0.90° . To obtain higher detail, the tail segments were scanned at a voxel resolution of $6.84\ \mu\text{m}^3$ and exposure time 2.1 s with a rotation step of 0.45° . These protocols produced serial cross-sectional 1024×1024 pixel images. These image files were cropped in Scion Image, beta 4.0.2 (Scion Image Corp., Frederick, MD, USA) and then exported to Analyze 4.0 (Mayo Clinic, Rochester, MN, USA) for volume rendering. Median filtration was used to reduce image noise and improve 3-D visualization of joint structures.

RESULTS

The limbs and proximal tails of 4 *ank/ank* female mice, 4 months of age, were subjected to μ CT to obtain the representative images depicted in Figures 1 through 6. Control images shown were derived from 2 age and sex matched mice. In addition, the joints of 4 additional female controls, aged 7–13 months, were examined (data not shown). In no instance did any of the control mice examined exhibit any of the musculoskeletal abnormalities evident in the *ank/ank* mutant.

Distal extremities. As seen in Figure 1, 3-D μ CT imaging revealed advanced bony ankylosis of all the joints of the carpus and paw of the *ank/ank* mouse, with the digits fixed in a hyperextended position. Both the distal and proximal interphalangeal joints were obliterated, being largely encased by calcified soft tissue. The metacarpophalangeal joints were fused, and the distal condyles of the metacarpals were enlarged and fused with their associated sesamoid bones. Although the latter had been largely assimilated into the calcified mass surrounding the metacarpophalangeal joints, they also appeared to be grossly enlarged (compare C and D, Figure 1). The metacarpal bone shafts were thickened, likely due to periosteal new bone formation and/or soft tissue calcification, a process that is also strikingly evident in the distal radius and ulna of the *ank/ank* mouse. Indeed, the space between these 2 bones has been obliterated by soft tissue calcification. The carpus of the *ank/ank* was an amorphous calcified mass fused to the ends of the radius and ulna, associated with an extension deformity of the paw. Changes in the hindlimb (Figure 2), while possibly somewhat less severe, mirrored those of the forelimb, including the presence of bony ankylosis of the digits and tarsus in a hyperextended position.

Elbows. The radius and ulna of the *ank/ank* mouse were fused to the humerus in a position of flexion (Figure 3). Calcification was found to extend around the joint capsule both anteriorly and posteriorly, with the olecranon process being apparently encased posteriorly by the calcified joint capsule and other soft tissue structures. The humero-radial joint was extensively involved, as a result of a plaque of

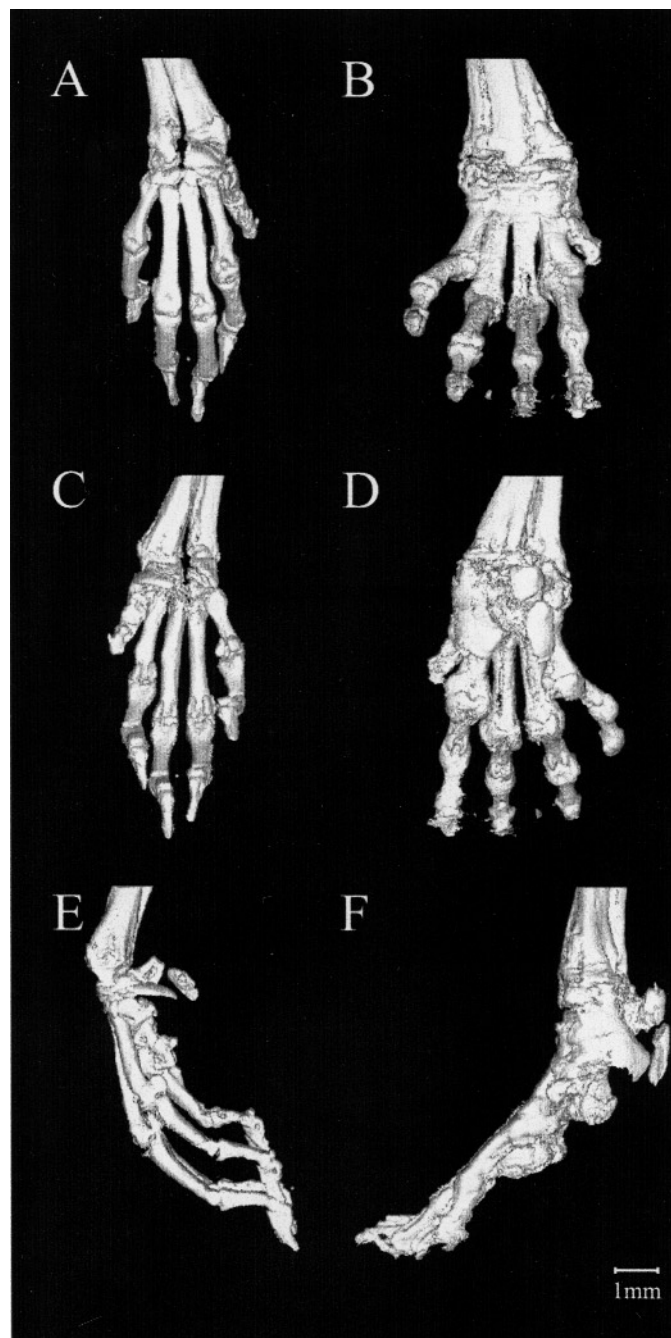


Figure 1. Representative μ CT reconstruction of the right distal forelimb from 4-month-old female control (left) and *ank* mutant (right) mice at 18 \times magnification. Dorsal (A, B), palmar (C, D), and medial (E, F) views are shown.

bone that incorporated the lateral sesamoid bone as well as the annular ligament (B and H, Figure 3). There was also a reduction in the size of the lateral supracondylar ridge of the humerus in an *ank/ank* animal as compared to a control mouse, best seen in the anterior (A, B) and posterior (C, D) views of the elbow in Figure 3. The medial epicondyle was less involved, but appeared enlarged by the addition of irregular nodular masses of new bone. The humeral trochlea

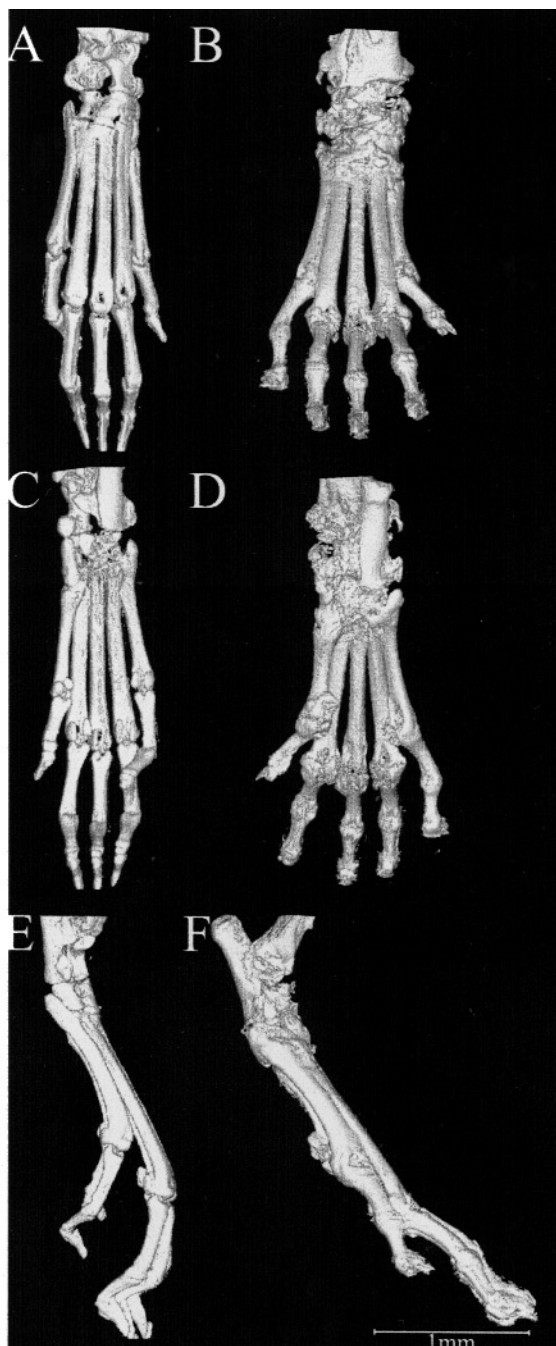


Figure 2. Representative μ CT reconstruction of the right distal hindlimb from 4-month-old control (left) and *ank* mutant (right) female mice at 18 \times magnification. Dorsal (A, B), plantar (C, D), and medial (E, F) views are shown.

and semilunar notch of the ulna were extensively involved by proliferation of new bone at the margins of the joint surface. In one *ank/ank* specimen, the bony enlargement of the ulnar coronoid process had produced notching of the humerus (data not shown). The radius and ulna were fused proximally in the region of the radial neck, and also more

distally, along the interosseous membrane, as shown in Figure 3 (E, F).

Knees. Changes in the knee of *ank/ank* mice were most pronounced in the menisci and the patella (Figure 4). Both menisci appeared enlarged as a result of extensive calcification (best seen in the anterior views, Figure 4, A and B) and in some cases these were fused together. This, perhaps in combination with chondrocalcinosis, resulted in an apparent narrowing of the joint space; however, fusion between the femur and tibia was not observed. The posterior views (C and D, Figure 4) demonstrate the proliferation of subchondral bone and/or chondrocalcinosis that have resulted in the loss of femoral condyle surface integrity. The size of the patella was increased due to calcification, a process that was also visible within the quadriceps tendon of some mice (B and F, Figure 4). In several cases the patella became fused to the patellar groove of the femur. As seen in the distal extremity sesamoid bones, the 2 posterior sesamoids underwent irregular enlargement due to new bone formation. Additional changes in the knee included the enlargement of the proximal tibia and the formation of calcified nodules, possibly osteophytes, on the lateral epicondyle of the femur, and within the intercondylar groove of the femur (Figure 4).

Proximal tail vertebrae. Changes observed in the proximal tail involved the fusion of vertebral elements (Figure 5). These included primarily the calcification of ligamentous structures concentrated around the annulus fibrosus. Thus the intervertebral space appeared highly irregular due to the formation of calcified nodules around the joint capsule; however, at least at this stage in the disease, the intervertebral disks were free of detectable calcification (Figure 6). While the articular processes (pre- and post-zygapophyses) were enlarged, the transverse processes were reduced in size relative to the control group. On the inferior surfaces, the hemal processes were considerably enlarged as were the adjacent sesamoid bones.

DISCUSSION

Having great potential for applications in skeletal analysis, μ CT is an emerging technology that can yield qualitative and quantitative information about gross morphology, as well as microstructural architecture. This technology offers numerous advantages, including its ability to rapidly generate geometrically accurate representations of sample morphology⁶. While previously limited by resolution to the study of larger animals^{3,4}, current capabilities of scan resolutions as small as 5 μ m have made it possible to study smaller animal models such as rats and mice^{5,6,8}. The capability of capturing images at such high resolutions not only allows for minute changes in the bone to be tracked^{5,9}, but also may permit smaller sample sizes to be used in order to reach significance⁹.

Consistent with previously described histopathological

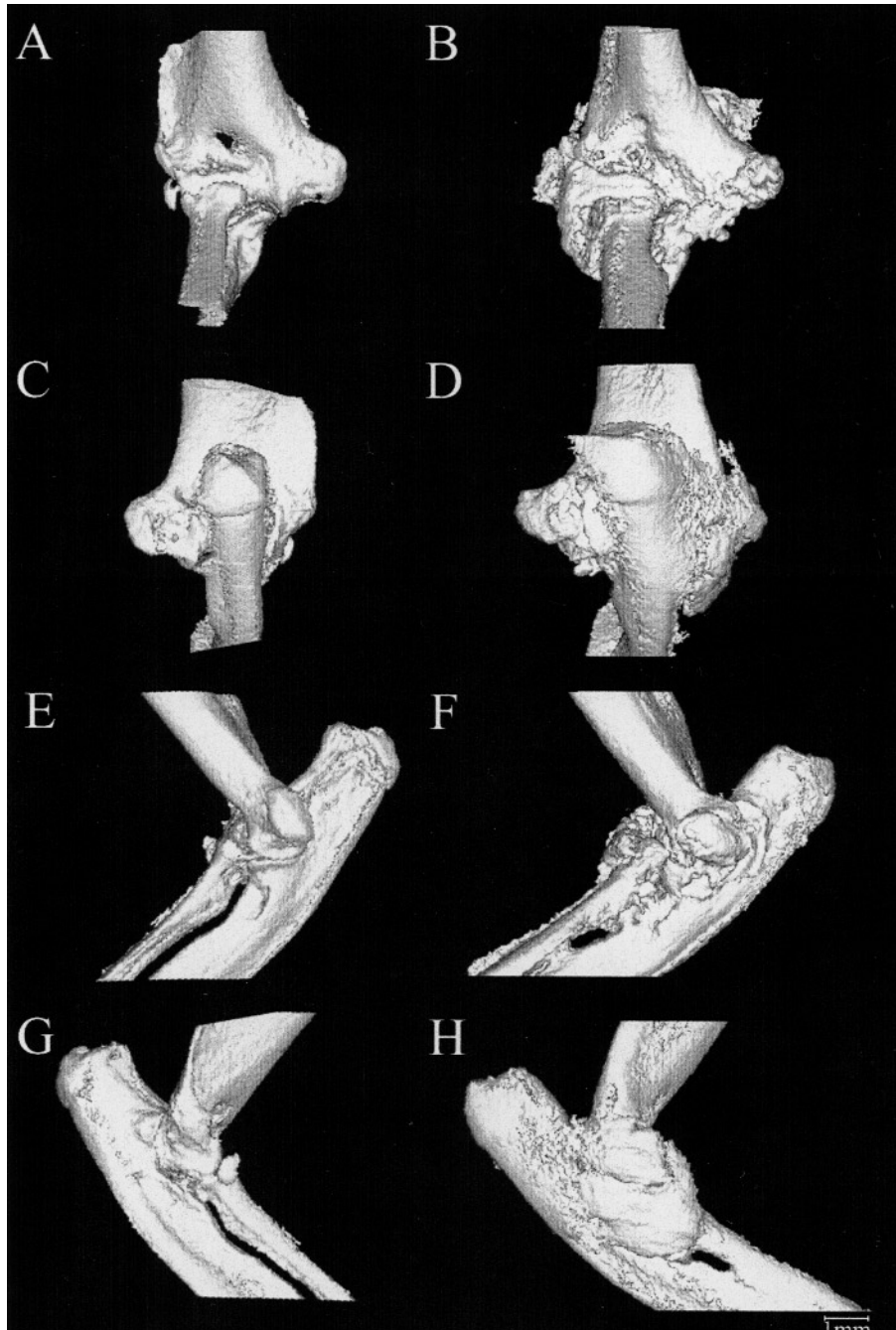


Figure 3. Representative μ CT reconstruction of the right elbow joint from 4-month-old normal (left) and *ank* mutant (right) female mice at 18 \times magnification. Anterior (A, B), posterior (C, D), medial (E, F), and lateral (G, H) views are shown.

findings^{1,2,12}, it is likely that the changes identified in the *ank* mouse by μ CT imaging consisted of a combination of soft tissue calcification as well as bony overgrowth of joint structures, including sesamoid bones, joint capsules, and ligaments. A prominent example of the latter was the calcified annular ligament around the head of the radius (Figure 3). Our findings correlate well with those previously

described using histology, alizarin staining, and radiography^{1,11,12}. The gradual process of ankylosis was also manifested by what appeared to be changes secondary to joint fusion and corresponding muscle disuse. Such secondary skeletal changes were most clearly observed in the elbow, where sites of tendinous attachment to bone were atrophic (data not shown). Other sites of what was likely secondary

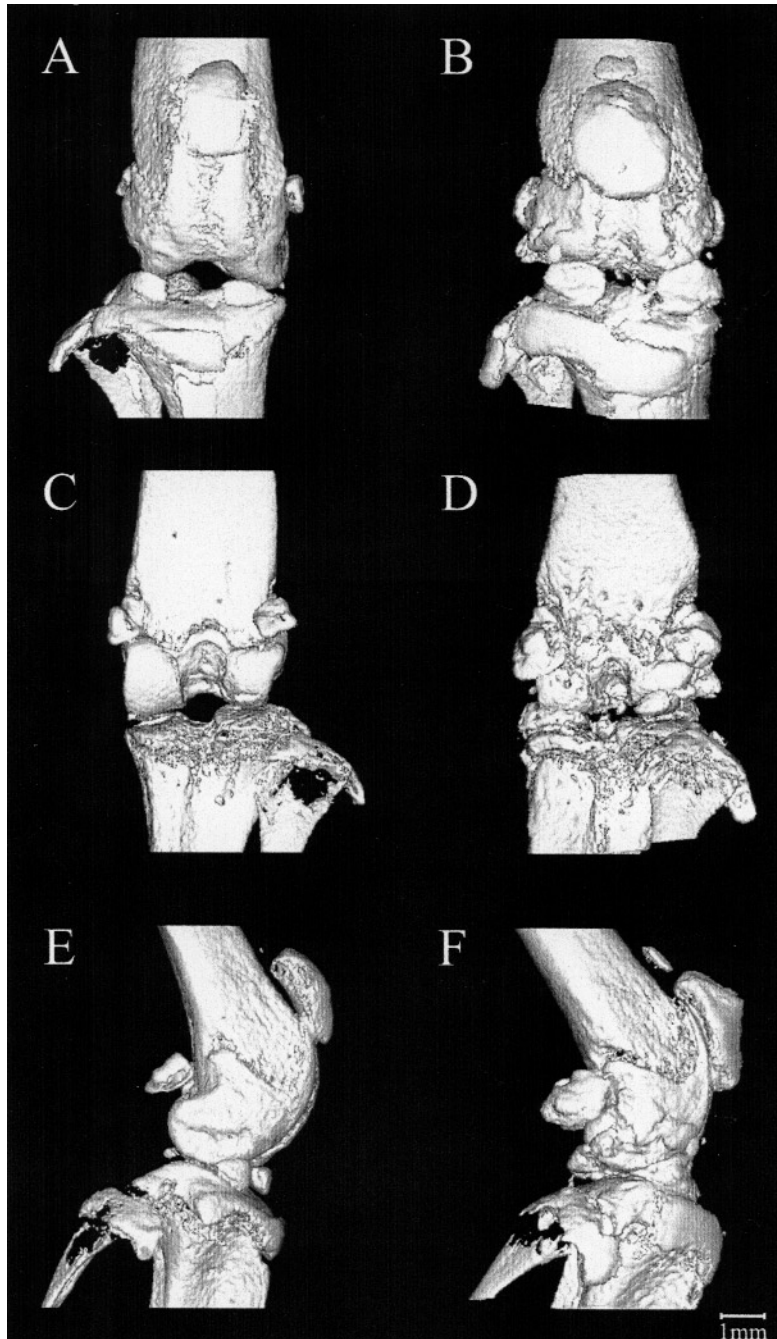


Figure 4. Representative μ CT reconstruction of the right knee from 4-month-old normal (left) and *ank* mutant (right) female mice at 18 \times magnification. Anterior (A, B), posterior (C, D), and lateral (E, F) views are shown.

change were found in non-joint structures such as the transverse processes of the caudal vertebrae, and notably, the lateral supracondylar ridge of the humerus (Figure 3). The reduction in size of these muscle insertion points was likely the result of decreased mechanical induction of bone growth as a result of joint ankylosis. Sweet and Green¹ found that *ank* mice tended to weigh less than normal littermates, and

that these weight differences were detected prior to overt joint fusion. This finding was interpreted to be indicative of reduced muscle mass resulting from decreased activity, initially due to joint pain, and subsequently, to limitation of joint movement. μ CT is ideally suited for the detection of subtle alteration in skeletal architecture, as illustrated by the ability to readily visualize secondary changes in bone struc-

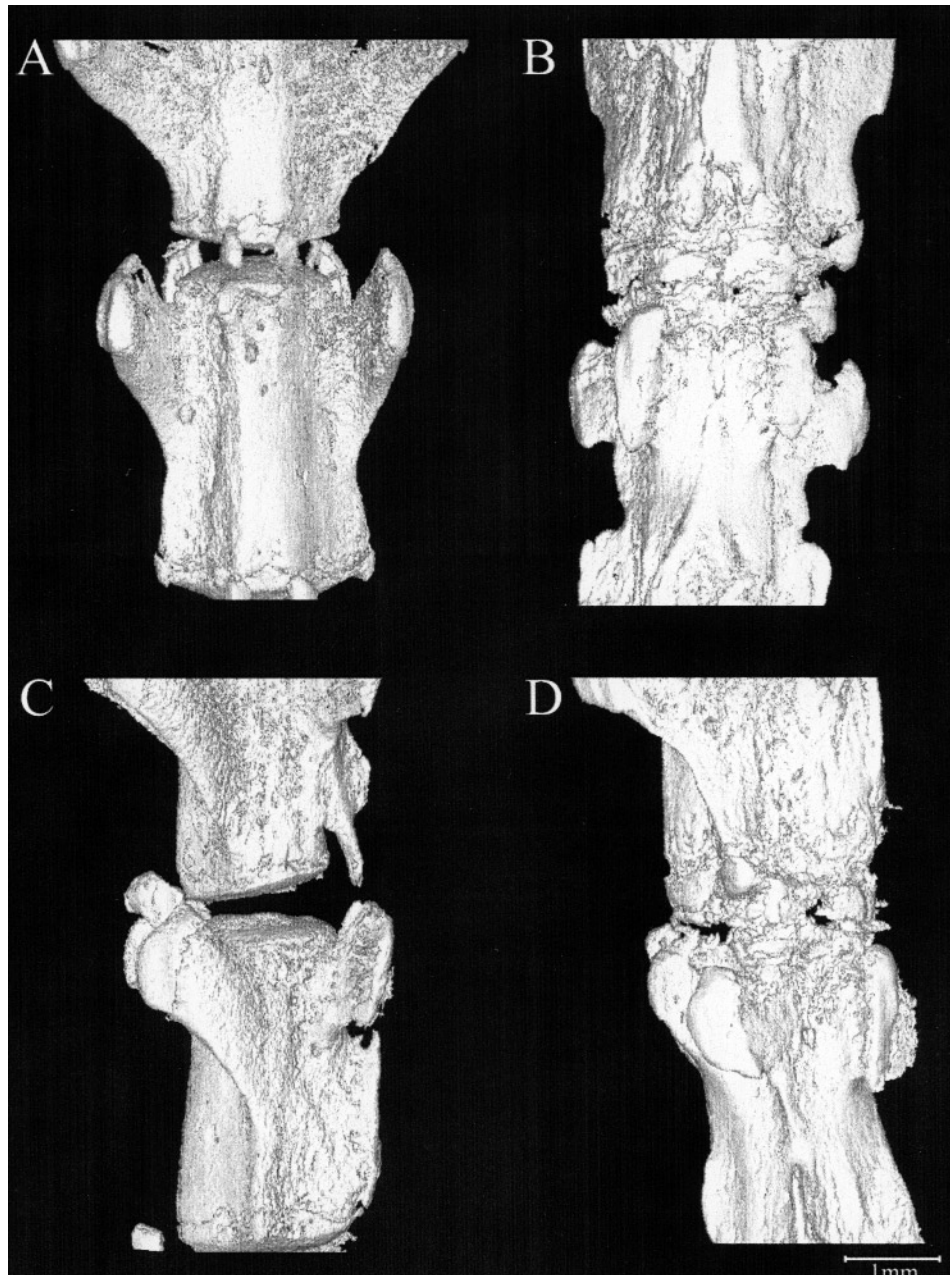


Figure 5. Reconstruction of the intervertebral space between 3rd and 4th caudal vertebrae of representative 4-month-old female normal (left) and *ank* mutant (right) mice at 40 \times magnification. Inferior (A, B) and lateral (C, D) views are shown.

ture at the points of muscle insertion in the *ank* mice. Revealing such changes would not be so easily achieved by conventional radiological or histological methods.

The ability to isolate and visualize skeletal elements in 3 dimensions offers a new means of assessing phenotypic alterations in mutant mice. This technology represents an intermediate level of evaluation lying between gross inspection and histological analysis that is not achievable with other techniques. Histology, for example, allows the visual-

ization of microscopic detail, including cellular changes, but is restricted to 2-D sampling of 3-D structures. μ CT provides a means of evaluating internal and external anatomical features in 3-D without the need for physical disruption of the sample. Thus, in this study, joint integrity remained unaltered, allowing a better understanding of the phenotypic changes associated with the *ank* mutation.

Despite its many positive features, μ CT has some limitations; these include the current inability to visualize changes

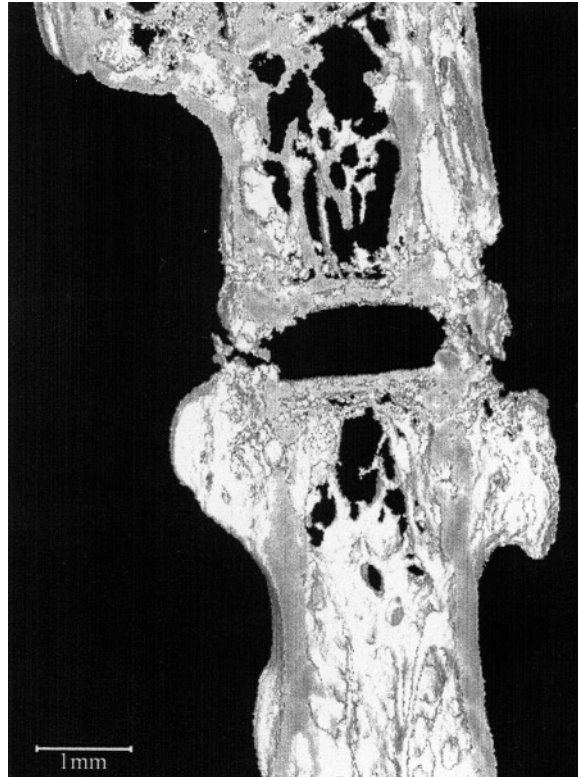


Figure 6. Mid-sagittal section of a representative μ CT reconstruction of the intervertebral space of the 3rd caudal vertebra, shown at 40 \times magnification.

in nonmineralized tissue, and also the inability to resolve cellular detail. For this reason, μ CT should be considered complementary to existing approaches. A notable advantage of μ CT in this regard is that it allows additional forms of analysis to be carried out on the same specimen, as the samples are not altered during the scanning process. While the results of the qualitative study described here show the utility of μ CT for descriptive types of analyses, future work will focus on developing the quantitative aspects of the technology. This includes examination of the external morphology of joints by 3-D landmarking (for example, to be able to discern volumetric changes in specific joint structures), and also internal morphology through the use of 3-D

architectural analysis of trabecular bone. These measurements will allow more quantitative characterizations of pathological states and disease progression.

ACKNOWLEDGMENT

We thank S. Lines and J. Gorday for help with the *ank* animal colony.

REFERENCES

1. Sweet HO, Green MC. Progressive ankylosis, a new skeletal mutation in the mouse. *J Hered* 1981;72:87-93.
2. Ho AM, Johnson MD, Kingsley DM. Role of the mouse *ank* gene in control of tissue calcification and arthritis. *Science* 2000;289:265-70.
3. Ito M, Nakamura T, Matsumoto T, Tsurusaki K, Hayashi K. Analysis of trabecular microarchitecture of human iliac bone using microcomputed tomography in patients with hip arthrosis with or without vertebral fracture. *Bone* 1998;23:163-9.
4. Kapadia RD, Stroup GB, Badger AM, et al. Applications of micro-CT and MR microscopy to study pre-clinical models of osteoporosis and osteoarthritis. *Technol Health Care* 1998;6:361-72.
5. Abe S, Watanabe H, Hirayama A, Shibuya E, Hashimoto M, Ide Y. Morphological study of the femur in osteopetrotic (*op/op*) mice using microcomputed tomography. *Br J Radiol* 2000;73:1078-82.
6. Graichen H, Lochmuller EM, Wolf E, et al. A non-destructive technique for 3-D microstructural phenotypic characterisation of bones in genetically altered mice: preliminary data in growth hormone transgenic animals and normal controls. *Anat Embryol Berl* 1999;199:239-48.
7. Cindik ED, Maurer M, Hannan MK, et al. Phenotypical characterization of *c-kit* receptor deficient mouse femora using non-destructive high-resolution imaging techniques and biomechanical testing. *Technol Health Care* 2000;8:267-75.
8. Yamashita T, Nabeshima Y, Noda M. High-resolution micro-computed tomography analyses of the abnormal trabecular bone structures in *klotho* gene mutant mice. *J Endocrinol* 2000;164:239-45.
9. McLaughlin F, Mackintosh J, Hayes BP, et al. Glucocorticoid-induced osteopenia in the mouse as assessed by histomorphometry, microcomputed tomography, and biochemical markers. *Bone* 2002;30:924-30.
10. Kapadia RD, Badger AM, Levin JM, et al. Meniscal ossification in spontaneous osteoarthritis in the guinea-pig. *Osteoarthritis Cartilage* 2000;8:374-7.
11. Sampson HW. Spondyloarthropathy in progressive ankylosis (*ank/ank*) mice: morphological features. *Spine* 1988;13:645-9.
12. Mahowald ML, Krug H, Halverson P. Progressive ankylosis (*ank/ank*) in mice: an animal model of spondyloarthropathy. II. Light and electron microscopic findings. *J Rheumatol* 1989;16:60-6.